Accepted Manuscript

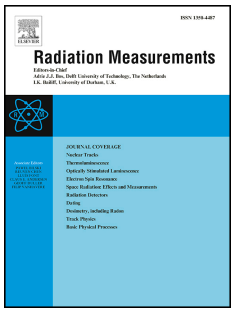

Effect of Spectrum Processing Procedure on the Linearity of EPR Dose Reconstruction in Tooth Enamel

D.V. Ivanov, A. Wieser, E.A. Shishkina, V.V. Ustinov

PII: S1350-4487(14)00190-5

DOI: 10.1016/j.radmeas.2014.06.008

Reference: RM 5268

To appear in: *Radiation Measurements*

Received Date: 24 June 2013

Revised Date: 29 May 2014

Accepted Date: 24 June 2014

Please cite this article as: Ivanov, D.V., Wieser, A., Shishkina, E.A., Ustinov, V.V., Effect of Spectrum Processing Procedure on the Linearity of EPR Dose Reconstruction in Tooth Enamel, *Radiation Measurements* (2014), doi: 10.1016/j.radmeas.2014.06.008.

Effect of Spectrum Processing Procedure on the Linearity of EPR Dose Reconstruction in Tooth Enamel

Ivanov D. V.[a, d], Wieser A.[b], Shishkina E. A.[c], Ustinov V. V.[a]

[a]*Institute of Metal Physics, Urals Division of Russian Academy of Sciences, 18, S. Kovalevskaya Str, 620990, Yekaterinburg, Russia.*

[b]*Helmholtz Zentrum München - German Research Centre for Environmental Health, D-85764, Neuherberg, Germany*

[c]*Urals Research Center for Radiation Medicine, 68A, Vorovsky Str, 454076, Chelyabinsk, Russia*

[d]*Ural Federal University, 19 Mira Str, 620002, Yekaterinburg, Russia.*

Abstract

Electron Paramagnetic Resonance (EPR) spectroscopy with tooth enamel is a widely used method of dosimetry. The accuracy of EPR tooth dosimetry depends on the spectrum processing procedure, the quality of which, in its turn, relies on instrumental noise and the signals from impurities. This is especially important in low-dose evaluation. The current paper suggests a method to estimate the accuracy of a specific spectrum processing procedure. The method is based on reconstruction of the radiation-induced signal (RIS) from a simulated spectrum with known RIS intensity. The Monte Carlo method was used for the simulations. The model of impurity and noise signals represents a composite residual spectrum (CRS) obtained by subtraction of the reconstructed RIS and the native background signal (BGS) from enamel spectra measured in HMGU (Neuherberg, Germany) and IMP (Yekaterinburg, Russia). The simulated spectra were deconvoluted using a standard procedure. The method provides an opportunity to compare the simulated "true" RIS with reconstructed values. Two modifications of the EPR method were considered: namely, with and without the use of the reference Mn^{2+} signals. It was observed that the spectrum processing procedure induces a nonlinear dose response of the reconstructed EPR amplitude when the height of the true RIS is comparable with the amplitudes of noise-like random splashes of CRS. The area of nonlinearity is below the limit of detection (DL). The use of reference Mn^{2+} signals can reduce the range of nonlinearity. However, the impact of the intensities of CRS random signals on nonlinearity is two times higher than the one observed when the reference signals were not used. The reproducibility of the software response is also dependent on both the amplitude of the CRS and the use of a reference signal, and it is also two times more sensitive to the amplitude of the CRS. In most EPR studies, all of the data are used, even those for which the dose value is lower than the DL. This study shows that low doses evaluated with the help of linear dose-response can be significantly

overestimated. It is recommended that linear dose response calibration curves be constructed using only data above the DL. Data below the DL should be interpreted cautiously.

Keywords: Tooth enamel; EPR; Monte Carlo simulations; Spectrum processing

Abbreviations: Radiation induced signals (RIS); Background native signal (BGS); Composite residual spectrum (CRS); Coefficient of variation (CV); Detection limit (DL)

Corresponding author tel.: +7-343-3783579; fax: + 7-343-3745244.
E-mail address: deniv@imp.uran.ru.

1. Introduction

Radiation dosimetry is a component of the complex biophysical and epidemiological studies related to the morbidity and mortality risk for humans exposed to ionizing radiation. Electron Paramagnetic Resonance (EPR) dosimetry with tooth enamel is a method for evaluating the doses accumulated during lifetime; it is used for reconstruction of the radiation dose accumulated over a lifetime. Ionizing radiation produces free stable CO_2^- radicals in hydroxyapatite, which is the primary mineral of tooth enamel. EPR dosimetry is based on the measurement of the paramagnetic resonance response of the CO_2^- radicals in tooth enamel. The intensity of the EPR response is proportional to the amount of radiation-induced radicals; thus, it reflects the absorbed dose in a sample (Ikeya et al., 1984). Fig. 1 shows an example of the EPR spectrum of tooth enamel exposed to a dose of 10 Gy. At present, this method has been widely used in retrospective dosimetry (Ikeya, 1993).

Usually, the EPR signal amplitude-to-dose conversion is based on a linear approximation (Wieser et al., 2000). No EPR response saturation with dose is observed at doses up to a few kGy (Liidja and Wieser, 2002). However, in some publications related to EPR dosimetry, the nonlinearity of the EPR response at low doses has been reported (Chumak et al., 1999). Some authors suggest that the nonlinearity of dose response at low dose areas could be related to the presence of competing trapping or recombination centers in hydroxyapatite (Jonas and Marseglia, 1997). However, this phenomenon could also be related to the procedure of analyzing the noisy signals that are typical of weak radiation-induced signals (RIS).

Instrumental noise is an unavoidable component of spectroscopy. The shape of the spectrum is significantly affected by the native background component of tooth enamel (BGS); even after a long chemical treatment, it cannot be completely extracted from the enamel sample (Ivannikov et al., 2001). The BGS has some variation of shape and can be fitted only with some uncertainty. Moreover, biological hydroxyapatite can contain various impurities, including metal ions (Shishkina et al., 2002). Therefore, in addition to RIS and BGS, the EPR spectrum contains a superposition of the instrumental noise and impurity signals, which influence the spectrum processing quality. Various algorithms are applied to reconstruct the RIS by spectrum analysis (Pass and Shames, 2000, Koshta et al., 2000, Dubovsky and Kirillov, 2001; Ivannikov et al., 2010). Algorithms for deconvolution are most commonly used for the automation of spectrum processing in routine measurements. There are two modifications of the EPR dosimetric measurements that require different approaches to processing the spectrum. The first approach is based on the use of the Mn^{2+} hyperfine signals of a reference sample, which allows the position of the magnetic field to be defined (Nagy, 2010). Fig. 2 presents the spectrum of tooth enamel (exposed to 3.6 Gy) recorded together with an Mn^{2+}/ZnS reference using IMP equipment. The Mn^{2+} lines are broadened due to the high amplitude of magnetic field modulation necessary to register the enamel spectrum. However, for

some EPR spectrometers, recording a spectrum using reference samples is difficult due to technical limitations. The Mn^{2+} reference can be used when the reference sample is fixed in the microwave cavity with no change of its position relative to that of the enamel sample. When this is not possible (for example, when the equipment is not used exclusively for dosimetric purposes), the positions of the Mn^{2+} lines can vary relative to the RIS due to inhomogeneity of the magnetic field in the cavity. Moreover, the use a reference implies an increase of a field sweep and, consequently, an enhancement of spectral resolution. If resolution enhancement is not technically possible, the number of points in the informative part of the spectrum will be reduced. Furthermore, the placement of an additional sample containing Mn^{2+} in the cavity leads to a reduction in its quality factor and, consequently, in the sensitivity (Zhumadilov et al, 2005). In the second approach, no reference samples are used. In this case, the position of the radiation-induced EPR signal is determined either based on the measurements of the microwave frequency or using a criterion for the best fitting of the RIS. The first method uses one fitting parameter of signal intensity in the RIS reconstruction. The second method uses two free parameters (signal intensity and magnetic field position) for fitting the RIS.

The aim of this study was to estimate the influence of instrumental noise and noiselike EPR response to impurities on the accuracy of dose reconstruction for one- or two-parameter approaches to RIS reconstruction. To achieve this goal, a numerical experiment was performed. For this purpose, impurities and noise were simulated using a composite residual spectrum (CRS) obtained by subtraction of reconstructed RIS and BGS from a number of measured EPR spectra of tooth enamel. In addition to instrumental noise and response to impurities, the CRS contains some residuals of non-perfect fitting of RIS and BGS. The spectra simulating measurements with known results were convoluted from the simulated “true” RIS and randomly selected CRS. Then, they were subsequently deconvoluted for reconstruction of the RIS intensity using EPR-Dosimetry software (Koshta et al., 2000).

Two models of CRS were developed based on real spectra that were measured at the Institute of Metal Physics (IMP) and the Helmholtz Zentrum Muenchen (HMGU). These two research groups use different equipment and instrument settings (Volchkova et al., 2011), and their performances are very different (Wieser et al., 2008).

It should be noted that only the idealized situation was considered in the current study, where no BGS influence on the RIS is assumed. In other words, ideal samples with negligible BGS were simulated. Nevertheless, in real tooth enamel dosimetry, the BGS affects the RIS reconstruction, and this issue will be considered in the discussion section.

2. Material and methods

2.1. EPR dosimetry

EPR spectra of 52 teeth and 30 teeth were measured at IMP and HMGU, respectively. The teeth were extracted for medical reasons in dental clinics of the Southern Urals (Russia) and Germany. The spectra were used for modeling two sets of spectral noise typical of the methods with different performance parameters.

The EPR spectra at IMP were recorded using an ERS-231 X-band spectrometer (manufactured by the Academy of Sciences of the former German Democratic Republic, Berlin-Adlershof) equipped with a ZSX-18 cylindrical cavity. The parameters of the spectrum recording were as follows: 5 mT magnetic field sweep; 0.45 mT modulation amplitude; 13 mW incident microwave power; accumulation time equal to 69 seconds and 30 scans. The EPR spectra at HMGU were recorded with a Bruker ECS 106 X-band spectrometer. The parameters of the spectrum recording were as follows: 5 mT magnetic field sweep; 0.14 mT modulation amplitude, 25 mW incident microwave power; accumulation time 84 seconds and 40 scans. Three repeated measurements were performed for each sample, resulting in the collection of 156 and 90 EPR spectra at IMP and HMGU, respectively.

The sample preparation procedure was similar in both laboratories. Tooth enamel was separated from the dentine using ultrasound treatment in an aqueous solution of NaOH at a concentration of 20 mol/l and a temperature of 60°C. The masses of the tooth enamel samples prepared at IMP and HMGU were 100 ± 4 mg and 115 ± 3 mg, respectively.

The EPR spectra were processed using a computer deconvolution procedure with modified EPR-Dosimetry software (Koshta et al., 2000). A set of three Gaussian lines and two tabulated functions was used to simulate the spectrum. The tabulated functions were obtained from simulated powder EPR spectra (Moens et al., 1993). The BGS was modeled using two Gaussian lines with g-factors of 2.0051 and 2.0035 and line widths of 0.49 mT and 0.42 mT, respectively, and one simulated powder spectrum based on a Gaussian line shape with a g-factor of 2.0045 and a line width of 0.78 mT. The radiation-induced signal was modeled using one Gaussian line corresponding to a weak isotropic signal from CO_2^- radical (g = 2.0006, line width: 0.21 mT) and one tabulated function with two components, including an orthorhombic signal with Lorentzian line shape (g_x=2.0032; g_y=1.9972; g_z=2.0019 and line widths of 0.20, 0.21 and 0.2 mT, respectively) and a quasi-axial signal with a Gaussian line shape (g_x =2.0027; g_y =1.9972; g_z =2.0025 and line widths of 0.46, 0.38 and 0.22 mT, respectively). Details of the tabulated functions are described in Zdravkova et al. (2003). In addition to the nonlinear curve fitting, the linear baseline correction was made.

The EPR-Dosimetry software was modified to be able to process multiple spectra in automated mode. A new algorithm was added to find the value of the magnetic field (or g-factor) shift. The software finds the most probable value of the g-factor in the experimentally determined range of its

possible shift (±0.03). The most probable g-factor shift is selected from the set of results of linear deconvolutions obtained by spectrum fitting with consistently changing g-factor values (step=0.00001) using the criterion of a minimum χ^2 (Chernoff and Lehmann, 1954).

2.2. Model of the "true" radiation-induced signal

The analytical model of the "true" RIS was developed by best fitting of the experimentally obtained RIS induced by 10 Gy of gamma ray exposure (Fig. 1). The model represents a linear combination of the derivatives of 4 Gaussian (Eq. 1) and 4 Lorentzian (Eq. 2) lines with fixed shape parameters ***b***. The scale parameters in both equations are indicated as ***a***; ***g*** indicates the location parameters responsible for the line position.

$$y = a*(x-g)/b*\exp(-0.5*\left(\frac{x-g}{b}\right)^2) \quad (1)$$

$$y = \frac{a*(x-g)/b}{1+\left(\frac{x-g}{b}\right)^2} \quad (2)$$

The superposition of the 8 lines is the function *R (A, g_0, x)* of the true signal (Eq. 3) characterized by the true RIS amplitude *A* and a location parameter g_0. The variable *x* is the coordinate along the axis of a spectral scan ($x=h\nu/\mu_B B$). The parameters of the lines are listed in appendix A.

$$\sum_{i=1}^{8} f_i(a_i, b_i, g_i, x) = R(A, g_0, x) \quad (3)$$

The two models of RIS used in EPR-Dosimetry software and obtained by best fitting are in good agreement. However, because the true shape of the RIS is uncertain, the convolution procedure uses an RIS model different from those applied for the deconvolution.

2.3. Monte Carlo simulation of experimental EPR spectra

Simulations of measured spectra were performed by convolution of a deterministic model of the "true" RIS and stochastic modeling of the CRS. The model of the CRS was obtained by point-to-point subtraction of the BGS and RIS signals from the initial EPR spectrum that was deconvoluted by EPR-Dosimetry software (Fig. 3). As a result, 156 and 90 CRSs of noise were fixed in the static databases for IMP and HGMU, respectively.

Each of the spectra is defined within the range ***l*** corresponding to the width of the magnetic field sweep. Monte Carlo simulations were performed in two steps: 1) the random drawing of a CRS from the static database; 2) the random drawing of a location for "true" RIS g_j (Eq. 3) based on the assumption that this parameter is floating uniformly within an interval Δ chosen such that in the subsequent convolution, the RIS would completely fit into the interval *l* (Eq. 4).

$$g_j = g_0 - \Delta*(0.5 - rand[0;1]) \quad (4)$$

Then, the "true" signal with a randomly shifted location was combined with the randomly selected CRS. Because of the idealized situation considered in the current study, a BGS was not applied for Monte Carlo simulation of the experimental EPR spectra. The obtained spectrum was processed by the EPR-Dosimetry software twice: with the known location, $g_{deconv} = g_j$, and with the unknown one. In the second case, the program automatically fits g_{deconv} by selecting the most accurate fitting of the spectrum using an algorithm for minimization of the χ^2 value. As a result, two amplitudes, $a_{1,2}$, were reconstructed for each true amplitude A.

The true values of amplitudes A were consistently simulated from 0 to 30 au with a step of 0.01 au. Each simulation of the EPR measurement was based on the average of three repeated drawings of the same amplitude. In total, 1500 drawings were made for each of the "true" amplitudes, simulating the measurements of 500 samples with the same "true" dose.

It should be noted that the amplitudes are expressed in arbitrary units, which differ for different equipment. To make the results comparable, both true and reconstructed amplitudes (A and a) were converted into the corresponding doses (D and d), according to the calibration factor typical of each method (Wieser et al., 2008). Thus, all results are represented in dose units.

3. Results and discussion

3.1 Description of models for spectral noise

The distributions of the amplitudes in CRS for both laboratories are characterized by Gaussian distributions with zero mean values. Fig. 4 presents a comparison of amplitude distributions in CRS represented in dose units. As can be observed from Fig. 4, the widths of the distributions are not equal. The values of the standard deviations and 95th percentiles of the distributions are shown in Table 1. As can be observed from the table, the distribution of amplitudes in CRS at IMP is wider than that at HGMU by a factor of approximately 2.

The threshold is the quantity above which one can determine that the physical effect is present (a difference exists between the measurements of the blank and the RIS). The blank represents the spectrum of enamel that has never been exposed to radiation. The value of the radiation dose must exceed a certain threshold value to assume that the measured signal includes some information about the dose. This threshold is called the critical dose. In previous studies, the level of significance for the critical value was selected to be $\alpha = 0.05$ (Wieser et al., 2008, Fattibene et al., 2011). Assuming the noise corresponds to the blank amplitude, the 95th percentile of the CRS amplitude distribution should correspond to the critical dose value, as shown in Ivanov et al. (2011). It should also be taken into account that individual EPR doses are usually obtained by averaging the results of three repeated measurements. Therefore, the parameters of the amplitude distribution in CRS width

(σ_{single}) were recalculated to dose equivalent units for triple measurements (σ_{triple}) according to Eqn. (5). This was performed to make the results comparable to the estimates of the critical dose for EPR dosimetry.

$$\sigma_{triple} = \frac{\sigma_{\sin ngle}}{\sqrt{n}}, \qquad (5)$$

The critical doses obtained from the CRS (5th column in Table 1) were compared with critical values calculated in Wieser et al., 2008 based on a 90% prediction interval for weighted least-squares fitting of EPR signal-to-dose response curves. The variances of the EPR measurements (6th column in Table 1) were assumed as weight factors. As can be observed from the table, the 95th percentile of CRS amplitude distribution represented in dose equivalent units for triple measurements do not contradict the preliminarily estimated critical values of the methods. This fact indicates that the parameters of CRS distribution are important and can be used to estimate the critical values, for example, in cases where it is not possible to perform the calibration experiment described in Wieser et al., 2008.

3.2. Numerical experiment

The results of simulation of triple EPR measurements with spectrum processing based on the automatic fitting of one or two parameters are shown in Fig. 5. The dependence of the mean reconstructed dose on the true dose is shown in Fig. 5a and 5c for one- and two-parameter fittings, respectively. As can be observed at low doses in all cases, there is a deviation from linearity. The nonlinearity is more explicit for the IMP method than for the HMGU method. In the region of small true doses, the software response becomes constant (d_{const}), and it depends on the width of the amplitude distribution in the CRS and the number of fitting parameters. The maximal value of the true dose for which the mean reconstructed dose is equal to d_{const} is denoted as D_{const}. The next important parameter describing nonlinearity is the border of true doses above which the software response can be assumed to be linear (D_{lin}). The parameter was evaluated based on the following criterion: if for 3 nearest true values (D) the root mean square deviations (RMSD) of the simulated doses are larger than their standard deviations (Eq. 6), then the deviation of the mean reconstructed doses (d) from linearity is significant.

$$\left.\begin{aligned} RMSD_i &= \sqrt{\frac{\sum_{j=i-1}^{i+1}(D_j - d_j)^2}{3}} \\ Stdev_i &= Stdev(d_{i-1}, d_i, d_{i+1}) \end{aligned}\right\} \; RMSD_i \geq Stdev_i \Rightarrow significant\, deviation\, from\, linearity \qquad (6)$$

Another important characteristic of the quality of a measurement is its repeatability. The analogous characteristic in the numeric experiment was the reproducibility of true dose

reconstruction, and it was estimated as the coefficient of variation (CV) of 500 doses reconstructed for each of the true doses. Fig. 5b and 5d show the dependence of the CV on the true doses for one- and two-parameter fittings, respectively. Assuming the least acceptable repeatability as 30% (CV≤0.3), the minimal true doses that met this condition were calculated ($D_{repeatable}$). Table 2 summarizes the parameters describing the quality of the software response to the true dose.

As can be observed from Table 2, both the CRS (an inherent characteristic of the method) and the number of fitting parameters (determined by the use or non-use of a reference sample) influence the linearity and repeatability of RIS reconstruction. The average ratio between the parameters obtained by the different laboratories (different CRS) under similar fitting conditions is equal to 4. The average ratio between the parameters obtained by the same laboratory but under different fitting conditions is equal to 2. Thus, the effect of CRS is found to be approximately 2 times greater than the effect of the use of a reference sample. However, the difference between the results for one- and two-parameter fitting is still significant, but the use of a reference signal can improve the EPR dosimetry only if there are no instrumental limitations.

3.3. Discussion

In practice, IMP and HMGU used the method for reconstructing EPR spectra with two fitting parameters. The lower bounds of the dose response linearity evaluated for two-parameter fitting exceed the critical doses (Wieser et al., 2008), and on average, they are equal to 40 and 110 mGy for HMGU and IMP, respectively (Fig. 5c). The large difference between these values is caused by the different conditions of the EPR equipment. The spectrometer at IMP is considerably older than the one at HMGU (Ivanov et al., 2011). The deviation from linearity for low doses results in a significant dose overestimation. The algorithm with two-parameter fitting of the RIS includes selection of the RIS position by analyzing the EPR signals in the neighborhood of the expected position of *g*. The most probable RIS is selected from the set of possible candidates according to the χ^2 criterion. However, if the CRS is comparable in magnitude to the measurand, then the software may select an impurity signal or a random low frequency noise peak as RIS. Therefore, the constant software response, obtained for low values of true RIS, is close to the 95^{th} percentile of the CRS amplitude distribution recalculated for triple measurements (Table 1). This explains why at zeroing, the true dose of the simulated spectrum does not approach zero after dose reconstruction (Fig. 5 a, c).

Two estimates of the detection limits (DL) for the methods (Wieser et al., 2008) were performed based on 90% prediction intervals for least-squares fitting of EPR signal-to-dose response curves. The first one was performed by weighting the prediction intervals by the variances of the EPR measurements; the second one was implemented without weighting. The DLs were found to be equal to 56/188 mGy and 157/368 mGy for HMGU and IMP, respectively. The values before the slashes

correspond to the weighted estimates; the unweighted estimates are indicated after the slashes. As can be observed, the minimal estimates of the DL are lower than $D_{repeatable}$, and for IMP, they are lower than D_{lin}. The maximal estimates of the DL for both methods fall into the linear and well-repeatable dose ranges. Therefore, the proposed maximal estimate of the DL is preferable as a criterion of data reliability. On the one hand, the doses in the range between the critical and DL values provide certain useful information and can be used in common analysis; but on the other hand, they are not reliable for individual estimates. Dose values such as these are typically used in statistical population analysis. For example, according to individual EPR measurements, the members of the Techa River Cohort (Krestinina et al., 2005) were externally exposed to doses in the range from undetectable levels up to 2 Gy (Degteva et al., 2005). Estimation of the average doses for specific groups formed according to residence histories is conducted by pooling all available doses, including undetectable cases (Volchkova et al., 2011). In such tasks, accounting for the nonlinearity of method-specific low dose response is indispensable.

Development of calibration curves includes all measurement results, including those measured for unexposed samples. The RISs of such samples can be in the range of non-linearity, which can, in turn, result in underestimation of the calibration factor. Therefore, constructing the linear dose response calibration curve using only data above the DL is recommended.

The results reported herein describe the case when BGS influence on RIS reconstruction is negligible. Real enamel spectra unavoidably contain BGS, the parameters of which can vary significantly. The influence on RIS reconstruction of the presence of BGS and its tooth-to-tooth variation represents a separate task that requires additional study. Simple preliminary testing of the influence of BGS was performed by adding the BGS with the same parameters used in the deconvolution procedure (the approach of perfect BGS fitting) described in section 2.1 to the simulated spectra. The amplitude of the BGS was constant, and its magnitude was selected to be equal to the mean of the BGS amplitudes of the experimental spectra described in 2.1. Fig. 6 shows the result of RIS reconstruction in the presence of BGS. As can be observed from Fig. 6, the area of non-linearity becomes more evident due to the increased complexity of the spectrum with the BGS. It can be expected that the real tooth-to-tooth variability of BGS can additionally contribute to nonlinearity.

5. Conclusions

A. The nonlinearity of the EPR dose response can be caused by the procedure of spectrum processing, and it depends on two factors: (1) the height of the CRS amplitude distribution and (2) the use or non-use of a reference signal. The impact of the first factor is two times greater than that of the second.

B. The repeatability of the software response is also dependent on these two factors, and it is also 2 times more sensitive to the height of CRS amplitude distribution.

C. The region of nonlinearity of EPR dose response is below the detection limit of the method. Therefore, constructing the calibration curve for linear dose response using only the data above the DL is recommended. Doses measured below the DL may be overestimated and should be interpreted with caution.

Acknowledgements

This research was supported by the International Joint EC Project 249675 (SOLO), Russian-American Program 1.1, Presidium of the Russian Academy of Sciences (Project No.12-M-23-2054) and grant NSH-1540.2014.2.

References

Chernoff H., Lehmann E. L. 1954. The use of maximum likelihood estimates in $\chi 2$ test for goodness of fit. The Annals of Mathematical Statistics. 25, 579–586.

Chumak, V., Sholom, S., Pasalskaya, L., 1999. Application of High Precision EPR Dosimetry with Teeth for Reconstruction of Doses to Chernobyl Populations. Radiat. Prot. Dosim. 84, 515–520.

Degteva, M.O., Anspaugh, L.R., Akleyev, A.V., Jacob, P., Ivanov, D.V., Weiser, A., Vorobiova, M.I., Shishkina, E.A., Shved, V.A., Vozilova, A.V., Bayankin, S.N., Napier, B., 2005. Electron Paramagnetic Resonance and Fluorescence In Situ Hybridization-based investigations of individual doses for persons living at Metlino in the upper reaches of the Techa River. Health Phys. 88, 139-153.

Dubovsky, S., Kirillov, V., 2001. Reconstruction of individual absorbed doses by tooth enamel on the base of non-linear simulation of their EPR-spectra. Appl Radiat Isot. 54, 833–837.

Fattibene, P., Wieser, A., Adolfsson, E., Benevides, L.A., Brai, M., Callens, F., Chumak, V., Ciesielski, B., Della Monaca, S., Emerich, K., Gustafsson, H., Hirai, Y., Hoshi, M., Israelsson, A., Ivannikov, A., Ivanov, D., Kaminska, J., Ke Wu, Lund, E., Marrale, M., Martens, L., Miyazawa, C., Nakamura, N., Panzer, W., Pivovarov, S., Reyes, R.A., Rodzi, M., Romanyukha, A.A., Rukhin, A., Sholom, S., Skvortsov, V., Stepanenko, V., Tarpan, M.A., Thierens, H., Toyoda, Sh., Trompier, F., Verdi, E., Zhumadilov, K., 2011. The 4th international comparison on EPR dosimetry with tooth enamel. Radiat. Meas. 46, 765-771.

Ikeya, M., Miyajima, J, Okajima, S, 1984. ESR dosimetry for atomic bomb survivors using buttons and tooth enamel. Jpn. J. Appl. Phys. 23, 697- 699

Ikeya, M., 1993. New Application of Electron Spin Resonance — Dating, Dosimetry and Microscopy. World Scientific, Singapore.

Ivannikov, A. I., Sanin, D., Nalapko, M., Skvortsov, V.F., Stepanenko, V.F., Tsyb, A.F., Trompier, F., Zhumadilov, K., Hoshi, M., 2010. Dental enamel EPR dosimetry: comparative testing of the spectra processing methods for determination of radiation-induced signal amplitude. Health Phys. 98, 345–351.

Ivannikov, A.I., Tikunov. D.D., Skvortsov, V.G., Stepanenko, V.F., Khomichyonok, V.V., Khamidova, L.G., Skripnik, D.D., Bozadjiev, L.L., Hoshi, M., 2001. Elimination of the background signal in tooth enamel samples for EPR-dosimetry by means of physical–chemical treatment. Appl. Radiat. Isot. 55, 701–705.

Ivanov, D., Shishkina, E., Volchkva, A., Timofeev, Yu., 2011. Analysis of the EPR dosimetry method performance at IMP in a long-term study. ANRI, 66, 65-71 (in Russian).

Jonas, M., Marseglia, E., 1997. A computational model for the simulation of radiation-induced trap-filling in multicrystalline insulators. Radiat. Meas. 27 (2), 351–357.

Koshta, A.A., Wieser, A., Ignatiev, E.A., Bayankin, S., Romanyukha, A.A., Degteva, M.O., 2000. New computer procedure for routine EPR-dosimetry on tooth enamel. Description and verification. Appl. Radiat. Isot. 52, 1287–1290.

Krestinina, L.Y., Preston, D.L., Ostroumova, E.V., Degteva, M.O., Ron, E., Vyushkova, O.V., Startsev, N.V., Kossenko, M.M., Akleyev, A.V., 2005. Protracted radiation exposure and cancer mortality in the Techa River Cohort. Radiat Res. 164, 602-611.

Liidja, G.,Wieser, A., 2002. Electron paramagnetic resonance of human tooth enamel at high gamma ray doses. Radiat. Prot. Dosim. 101(1–4), 503–506.

Moens, P., De Volder, P., Hoogewijs, R., Callens, F., Verbeeck, R.,1993. Maximum-likelihood common-factor analysis as a powerful tool in decomposing multicomponent EPR powder spectra. J. Magn. Reson. 101, 1–15.

Nagy, V., 2000. Accuracy considerations in EPR dosimetry. Appl.Radiat.Isot. 52, 1039–1050.

Pass, B, Shames, A.I., 2000. Signal processing for radiation dosimetry using EPR in dental enamel: comparison of three methods. Radiat. Meas. 32, 163–167.

Shishkina, E.A., Shved, V.A., Tolstykh, E. I., Degteva, M.O., Anspaugh, L.R., 2002. Investigation of the tooth as a complex dosimeter: Formation of dose in tooth enamel. Chelyabinsk, Russia, and Salt Lake City, UT: Urals Research Center for Radiation Medicine and University of Utah, Unscheduled report.

Volchkova, A.Yu., Shishkina, E.A., Ivanov, D.V., Timofeev, Yu., Fattibene, P., Della Monaca, S., Wieser, A., Degteva, M.O., 2011. Harmonization of dosimetric information obtained by different EPR methods: Experience of the Techa river study. Radiat. Meas. 46, 801-807.

Wieser, A., Mehta, K., Amira, S., Aragno, D., Bercea, S., Brik, A., Bugai, A., Callens, F., Chumak, V., Ciesielski, B., Debuyst, R., Dubovsky, S., Duliu, O.G., Fattibene, P., Haskell, E.H., Hayes, R.B., Ignatiev, E.A., Ivannikov, A., Kirillov, V., Kleschenko, E., Nakamura, N., Nathe, M., Nowak, J., Onori, S., Pass, B., Pivovarov, S., Romanyukha, A., Scherbina, O., Shames, A.I., Sholom, S., Skvortsov, V., Stepanenko, V., Tikounov, D.D., Toyoda, S., 2000. The 2nd International Intercomparison on EPR Tooth Dosimetry. Radiat. Meas. 32, 549-557.

Wieser, A., Fattibene. P., Shishkina. E.A., Ivanov, D.V., De Coste, V., Guettler, A., Onori, S., 2008. Assessment of performance parameters for EPR dosimetry with tooth enamel. Radiat. Meas. 43, 731-736.

Zdravkova, M., Wieser, A., El-Faramawy, N., Ivanov, D., Gallez, B., Debuyst R., 2003. An in vitro L-band EPR study with whole human teeth in a surface coil resonator. Radiat. Meas. 37, 347–353.

Zhumadilov, K., Ivannikov, A., Skvortsov, V., Stepanenko, V., Zhumadilov, Z., Endo, S., Tanaka, K., Hoshi, M., 2005. Tooth enamel EPR dosimetry: optimization of EPR spectra recording parameters and effect of sample mass on spectral sensitivity. J. Radiat. Res. 46, 435–442.

Figure legends

Fig. 1. An EPR spectrum of tooth enamel irradiated at a dose of 10 Gy. On the upper abscissa, the value of the magnetic induction (B) is converted into units of the gyromagnetic ratio (g-factor = $h\nu/\mu_B B$). The bold line indicates the asymmetric resonance absorption peak resulting from CO_2^- radicals with g-factor components of $g_\perp$=2.0018 and $g_\parallel$=1.997. *A* is the amplitude of the $g_\perp$ signal component.

Fig. 2. An enamel spectra recorded together with an Mn^{2+} reference. The irradiation dose of the enamel sample was 3.6 Gy.

Fig. 3. An example of CRS obtained from EPR spectra measured at IMP. The dotted lines show the simulation of RIS and BGS. The irradiation dose of the enamel sample was 3.4 Gy.

Fig. 4. The distribution of CRS amplitudes for IMP (a) and HGMU (b). The bold line represents the curve of a normal distribution.

Fig. 5. The results of reconstruction of known doses from CRS and RIS combination for IMP and HMGU: a) mean values of 500 doses reconstructed for each true dose using one fitting parameter; b) coefficients of variation for doses reconstructed with one fitting parameter depending on the true dose; c) mean values of 500 doses reconstructed for each true dose using two fitting parameters; d) coefficients of variation for doses reconstructed with two fitting parameters depending on the true dose.

Fig. 6. The results of reconstruction of doses from CRS and RIS combination with BGS (empty points) and without BGS (filled points) using two fitting parameters (IMP data).

Appendix A

Table A.1. The parameters of Gaussians and Lorentzians used for simulation of “true” RIS in Monte-Carlo experiments. The ***g*** is the location parameter, and the ***b*** is the shape parameter.

Gaussian		Lorentzian	
g	***b***	***g***	***b***
2.00228	0.001088	2.0014114	0.0003075
2.004055	0.0009387	2.0018311	0.000249
2.005704	0.001311	2.0025674	0.0001747
2.0026328	0.00002505	2.00221288	0.000205

Table 1. Description of the width of spectral noise. Critical dose is shown according to Wieser et al. 2008.

	σ of noise distribution, mGy	σ of triple measurement, mGy	95th percentile of noise distribution, mGy	95th percentile of triple measurement, mGy	Critical dose*, mGy
IMP	110	70	170	100	93
HMGU	50	30	90	50	33

* The critical dose is the dose below which the confidence in the significance of the result is less than 5%.

Table 2. Parameters describing quality of software response to the true dose, mGy. The D_{lin} *is the bound of doses with linear software response, The* d_{const} *is the region of true doses with constant software response, the* D_{const} *is the maximal dose in* d_{const} *region, and* $D_{repeatable}$ *is the minimal true dose satisfying the repeatability of 30%.*

Parameter	HMGU		IMP	
	One-parameter fitting	Two-parameter fitting	One-parameter fitting	Two-parameter fitting
D_{lin}	30	60	170	250
D_{const}	<5	15	25	60
d_{const}	15	40	50	110
$D_{repeatable}$	60	90	230	290

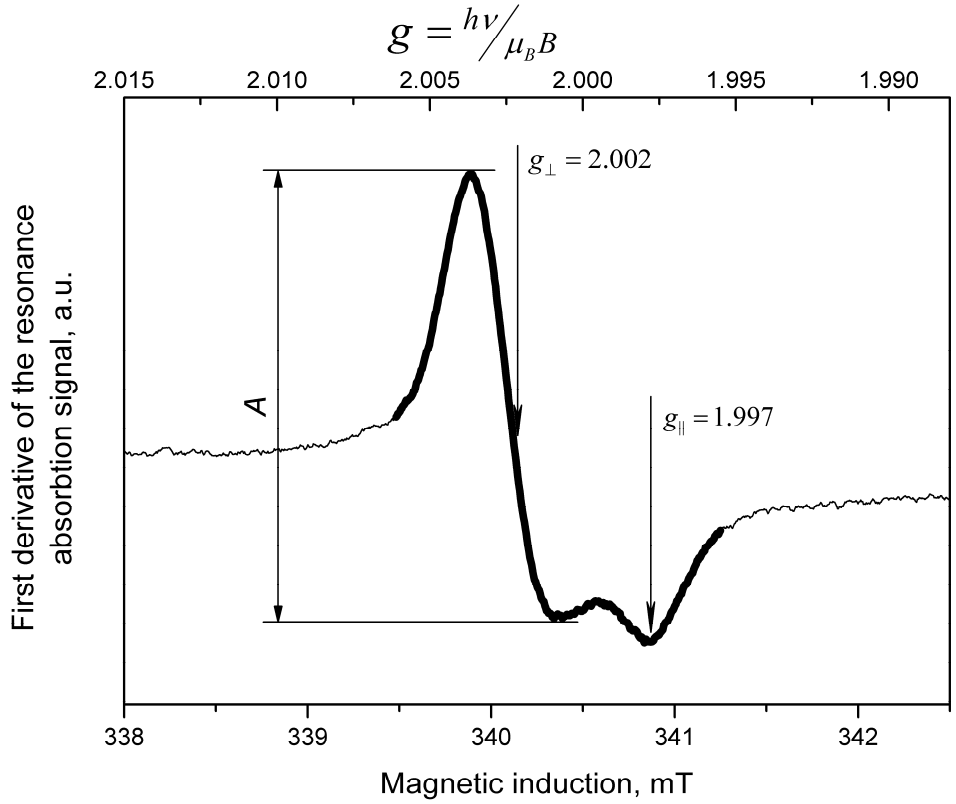

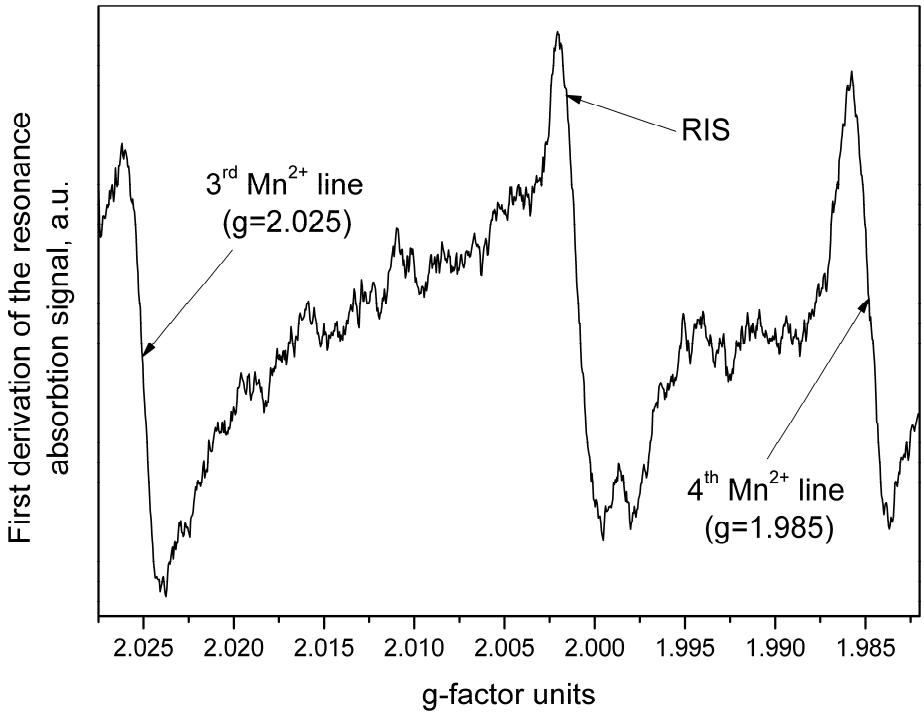

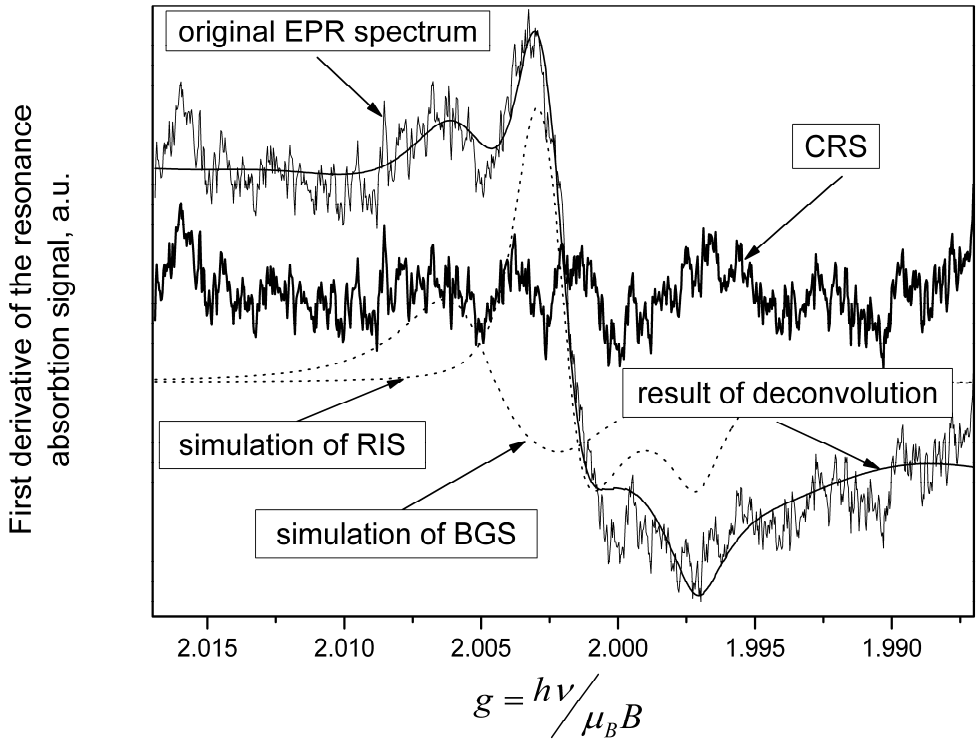

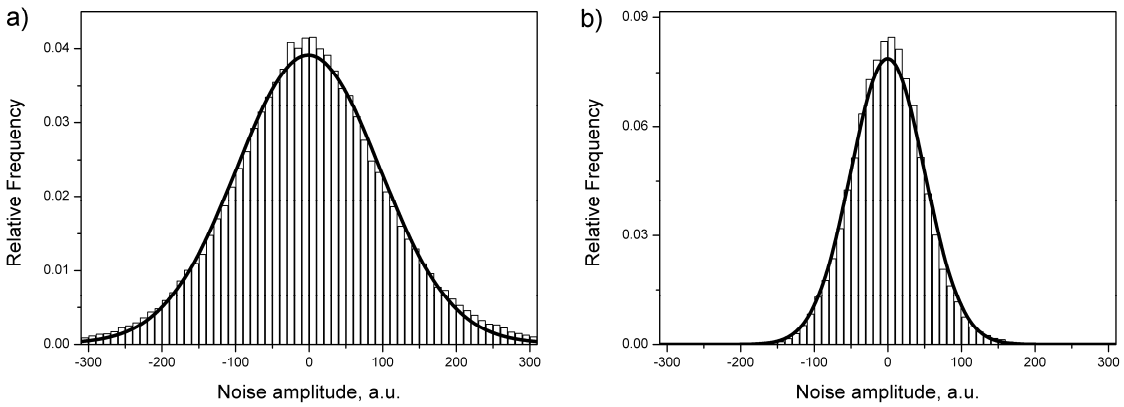

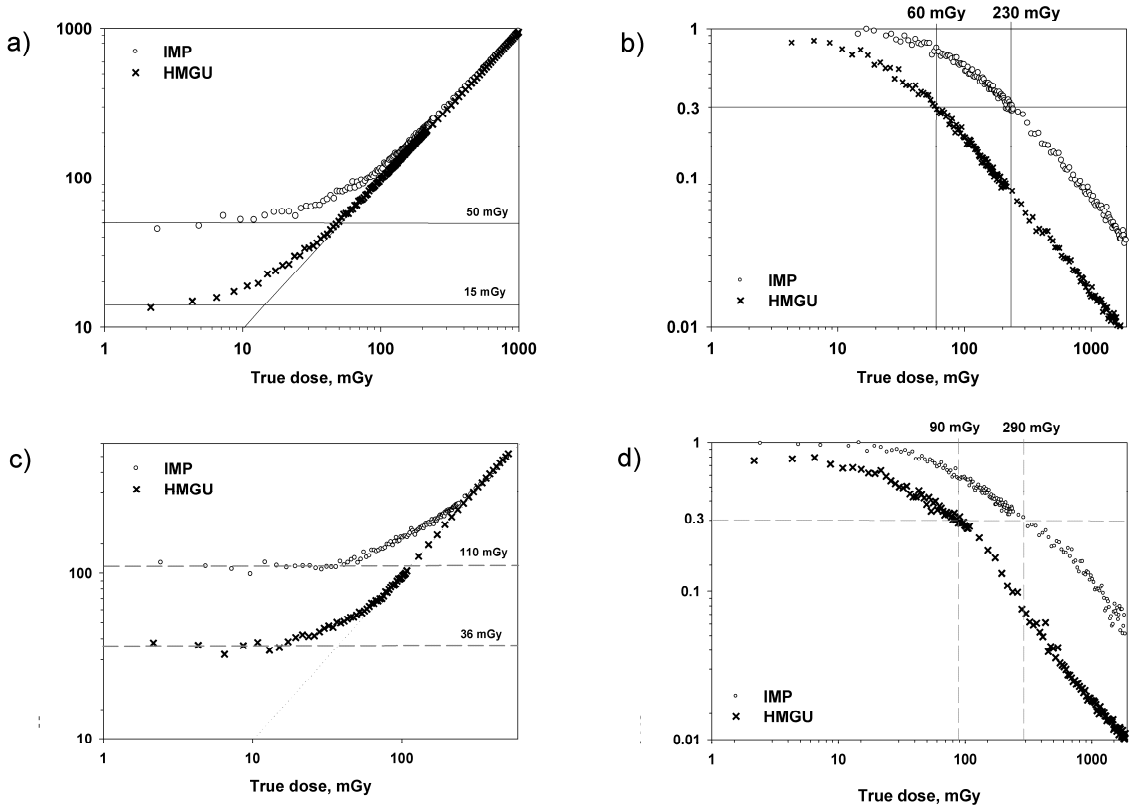

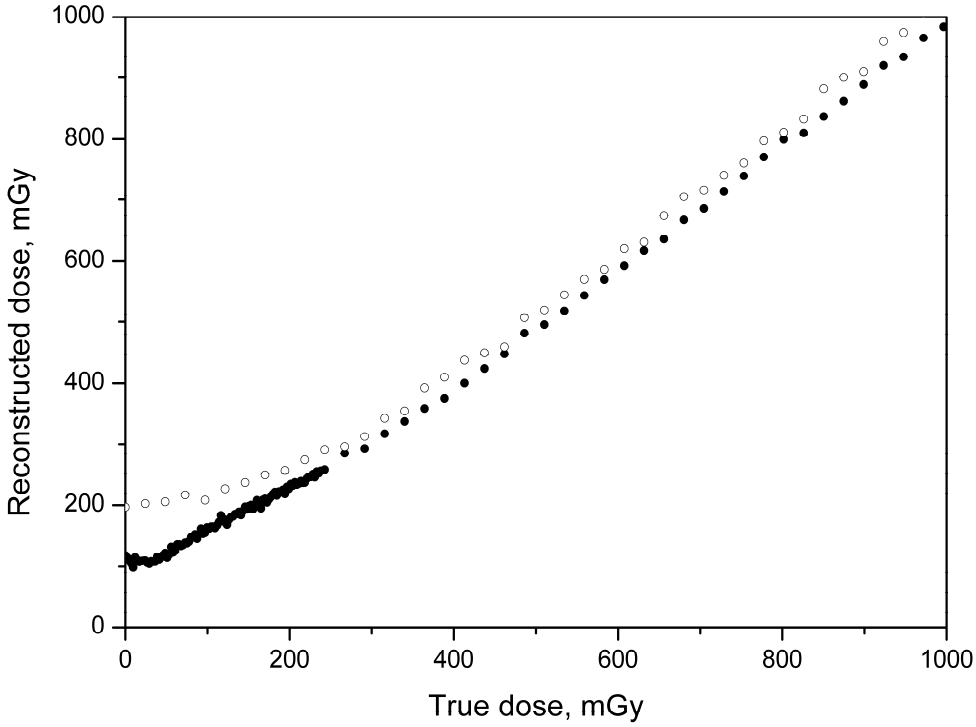

Highlights:

Spectrum processing causes a nonlinearity of the EPR response to low doses.

Parameters of nonlinearity depend mainly on the spectral noise height.

The nonlinearity area of EPR dose response is below the limit of detection.

Area of nonlinearity can be slightly reduced by applying a reference signal.

The repeatability of software response is dependent on spectral noise height.